Pergamon

Scripta Materialia, Vol. 40, No. 4, pp. 409–415, 1999
Elsevier Science Ltd

1359-6462/99/$–see front matter

PII S1359-6462(98)00444-8

CODEPOSITION OF NANOCRYSTALLINE $NbAl_3$ PARTICLES ON Cu

I. Manna, P.P. Chatterjee, V. Srinivas Rao and S.K. Pabi
Metallurgical and Materials Engineering Department, Indian Institute of Technology, Kharagpur 721 302 (W.B.), India

(Received September 30, 1998)
(Accepted in revised form November 12, 1998)

Introduction

Copper is widely used as an electrical and thermal conductor due to its very high conductivity [1]. However, pure Cu possesses poor wear and oxidation resistance which poses difficulties like arcing and short circuiting in electrical contacts. Addition of Sn, Zn, A1, etc. to the bulk is known to improve the wear and oxidation resistance of Cu, though, deteriorating the conductivity of Cu in the process. However, wear and oxidation are surface dependent properties [2]. Therefore, a suitable modification of the surface chemistry and microstructure of the Cu based conductors may achieve the required protection against wear and oxidation without deteriorating the electrical and thermal conductivity of Cu. Recently, attempts have been made to introduce Cr on the surfaces of Cu by laser surface alloying to enhance the wear resistance of the substrate [3]. In contrast to the thermal processes, electrochemical codeposition of ceramic particles on metal surface has recently been attempted as a novel technique in surface engineering [4]. In the present study, we shall report a similar effort for the first time to enhance the wear resistance of Cu by codeposition of hard ultrafine intermetallic particles along with electrodeposition of Cu on pure Cu substrates. It is expected that the present method will achieve a better microstructural and compositional homogeneity in the deposited layer than that in the alloyed zone produced by the line of sight process of laser surface alloying.

Experimental

Nanocrystalline $NbAl_3$ powders were prepared by mechanical alloying of high purity (>99.5 wt.%) elemental powders of Nb (100 μm) and A1 (50 μm) taken in the atomic ratio of 3:1 suspended in toluene in a high energy Pulverisette-5 (Fritsch) planetary ball mill. The milling was carried out at 300 rpm in WC coated vials using 10 mm diameter balls with similar coatings with a ball to powder weight ratio of 10:1. Milled powder samples were collected from the vial at predetermined intervals to determine the chemistry and average crystallite size (d_c) of the milled product through peak broadening analysis by x-ray diffraction (XRD) using a Philips PW1840 machine using Co-K_α radiation. The respective contribution of strain and instrumental errors on peak broadening were duly considered and eliminated while calculating the value of d_c [5]. Ball milling was continued until all the diffraction peaks of the constituent elements disappeared from the XRD profile and d_c of $NbAl_3$ reached a value of $\leq$ 20 nm.

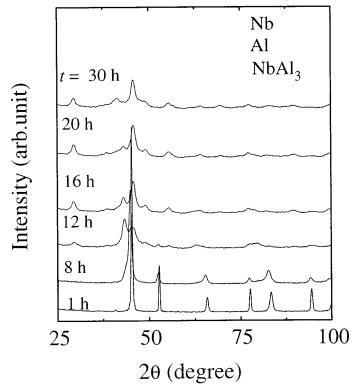

Figure 1. A series of XRD patterns obtained from a powder blend of $Nb_{25}Al_{75}$ following mechanical alloying for different periods of cumulative milling time (t).

The freshly milled and dried (in air to remove toluene) nanocrystalline $NbAl_3$ powders were dispersed in an aqueous electrolytic bath containing $CuSO_4$ (8 g/l) with a pH level of 3.5. The bath was used for codeposition of the colloidally suspended $NbAl_3$ nanoparticles along with electrodeposition of Cu on flat Cu plates. The electrodeposition was carried out at a d.c. potential of 3–5 volts applied between the Cu-cathode and Pt-electrode. The bath was maintained at 40°C using a thermostat. The uniformity of the colloidal dispersion of $NbAl_3$ was maintained by magnetic stirring (for 30 min) prior to and during electrodeposition. The process parameters varied were time (t), current (i) and dispersion density (w) of the $NbAl_3$ particles.

Following codeposition under predetermined routines, the samples were subjected to a detailed characterization of surface microstructure (by scanning electron microscopy, SEM), surface chemistry (by energy dispersive spectroscopy, EDS), and phase identity and distribution (by XRD analysis). Superficial hardness of the codeposited samples was determined by Vickers microhardness testing. Subsequently, a selected set of samples, prepared by codeposition of $NbAl_3$ with Cu on transparent silica substrates precoated with a thin (1 μm) Cu film by vapor deposition was subjected to electrical resistivity measurement by the four probe method using a d.c. double Kelvin bridge. Finally, an attempt has been made to correlate the conductivity and hardness with the microstructure and composition of the surface layer.

Results and Discussion

Preparation of $NbAl_3$

Figure 1 represents a series of XRD patterns obtained from an initial powder blend of $Nb_{23}Al_{77}$ (by atomic percent) milled for different periods of time. It is evident that the elemental powders (Nb and Al) continue to exist until about 16 h of milling albeit concomitant shift in the respective peak positions indicating mutual dissolution by mechanical alloying. It appears that $NbAl_3$ forms with 12 h of milling and attains a measurable volume fraction beyond 16 h of milling. It is interesting to note that appearance of $NbAl_3$ coincides with the disappearance of the XRD peak of Al. Eventually, the Nb peaks disappear beyond 20 h of milling. It may be noted that $NbAl_3$ formed here is an ordered intermetallic compound characterized by its (101) and (110) superlattice peaks. This is in accordance with an earlier study on mechanical alloying of Nb and Al [6]. The individual peaks register measurable broadening due to reduction in d_c size with an increase in the milling time. Figure 2 shows the variation of d_c obtained by

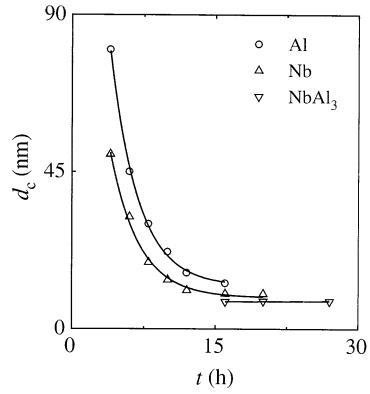

Figure 2. Variation of crystallite size (d_c) of Nb, Al and $NbAl_3$ (formed by mechanical alloying) as a function of cumulative milling time (t).

XRD peak broadening analysis using Scherrer's formula [7] as a function of milling time. It is evident that d_c of Nb and Al reduce to nanometric level within 3–5 h of milling. However, $NbAl_3$ forms only beyond a critical milling time and hence reduction of the concerned d_c of Nb and Al. It is interesting to note that d_c of $NbAl_3$ remain nearly identical during the entire course of milling since its formation.

Codeposition of $NbAl_3$

Initial trials in the present experiment reveal that the relative rate of deposition of Cu and codeposition of $NbAl_3$ are both crucial to obtain a smooth and adherent deposit layer on the surface. While the former is a function of i, the latter is determined by w. Therefore, w must have an upper limit for any given i, beyond which accumulation of excess $NbAl_3$ on the cathode may hinder the electrochemical process of ionic charge transfer between the cathode and Cu ions. Assuming a linear stacking of codeposited nanocrystalline and spherical $NbAl_3$ particles of 20 nm average grain diameter along the three mutually perpendicular directions with electrodeposited Cu atoms clustering in the voids left between the adjacent $NbAl_3$ particles (Fig. 3), the mass (m_{NbAl3}) of the codeposited particles is given by

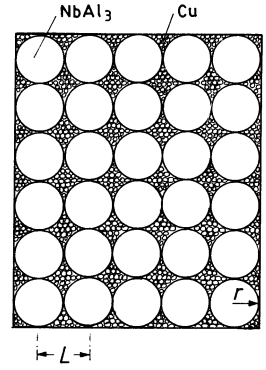

Figure 3. A schematic representation of the assumed distribution of codeposited nanocrystalline $NbAl_3$ particles in the electrodeposited Cu matrix.

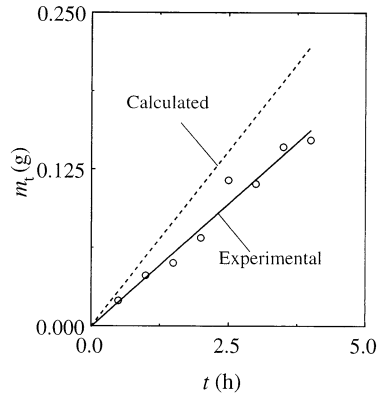

Figure 4. Variation of accumulated total mass (m_t) of electrodeposited Cu and codeposited $NbAl_3$ with electrodeposition time (t).

$$m_{NbAl_3} = \frac{4abc}{3L^3}\,\pi r^3\,\rho_{NbAl_3} \tag{1}$$

where a, b and c are dimensions of the deposited layer in three mutually perpendicular directions, r is the radius of $NbAl_3$ particles, L is the minimum interparticle separation such that $L = 2r$ and ρ_{NbAl3} is the density of $NbAl_3$. It may be noted that Fig. 3 represents the maximum possible density of packing of $NbAl_3$ particles and Cu atoms. Here, it is assumed that Cu is elecrodeposited only in the void spaces between the $NbAl_3$ particles on a given plane (Fig. 3). Thus, the mass of the deposited Cu (m_{Cu}) at the same time interval (t) is obtained as:

$$m_{Cu} = abc\left(1 - \frac{4}{3L^3}\,\pi r^3\right)\rho_{Cu} \tag{2}$$

Now, dividing equation (2) by equation (1), we get

$$\frac{m_{Cu}}{m_{NbAl_3}} = 1.8 \tag{3}$$

Therefore, equation (3) is useful to calculate the amount of $NbAl_3$ necessary for dispersion in the electrolyte for the densest possible codeposition. Accordingly, it is predicted that (8/1.8 = 4.4) g/l of $NbAl_3$ is required in the electrolyte containing 8 g/l of $CuSO_4$ (as is used for electrodeposition of Cu) for codeposition of $NbAl_3$ in the present investigation. While the Faraday's first law of electrochemistry yields: $m_{Cu} = Zit$, where Z is the electrochemical equivalent of Cu, equation (3) yields the value of m_{NbAl3} for the identical time interval assuming $L = 2r$ in equation (1). Figure 4 shows the variation of the predicted total mass gain ($m_t = m_{Cu} + m_{NbAl3}$) as a function of t due to electro/codeposition of as per equations (1)-(3). For a suitable verification, the experimentally determined values of m_t are also included in Fig. 4 obtained by calculation as well as experiment as a function of t. It appears that the experimental curve deviates from the calculated one with increase in time which may be attributed to the gradual dilution of Cu and $NbAl_3$ in the solution with the progress of electrodeposition.

Microstructure and Composition of Surface Deposit

Figure 5 reveals a typical micrograph of the surfaces of Cu substrates codeposited with $NbAl_3$ powders. It is evident that $NbAl_3$ is mostly deposited along the boundaries of electrodeposited Cu grains. Figure

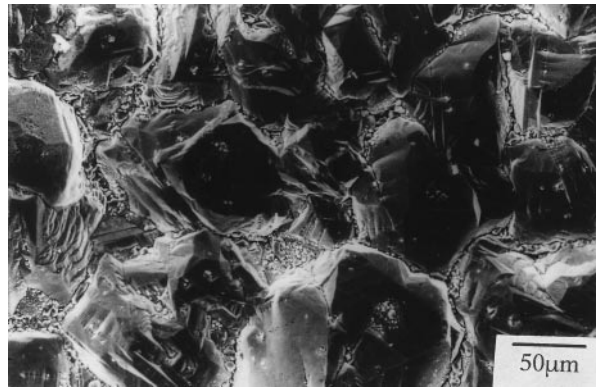

Figure 5. An SEM micrograph showing the codeposited ultrafine $NbAl_3$ particles along the grain boundaries of electrodeposited Cu. Codeposition was carried out with electrodeposition from a $CuSO_4$ solution (8 g/l and 3.5 pH) containing $w = 1$ of colloidally dispersed $NbAl_3$ particles at 4 V for $t = 200$ min.

6 evidences entrapment of $NbAl_3$ particles both along the grain boundaries and within the grain bodies. However, the $NbAl_3$ particles seem to agglomerate into coarser aggregate of nearly micrometer sizes during codeposition. A close scrutiny reveals that finer particles (<1 μm) are also embedded within the Cu grains on the codeposited surface (Fig. 7).

Figure 8 confirms the presence of $NbAl_3$ in the codeposited surface of Cu through an XRD pattern obtained from a codeposited sample. It may be noted that (111) is not the most intense peak for Cu here (as is expected in the XRD of pure Cu). This may be attributed to the influence of texture developed during the electrodeposition process. Furthermore, the relatively lower intensity of $NbAl_3$ peaks compared to those of Cu suggests that the former is present in the low volume fraction.

A selective EDS analysis reveals the presence of Cu, Nb, Al, Cr and Fe in randomly chosen areas of the surface deposits. Fe and Cr may be the impurities introduced during ball milling. A typical analysis result shows: Cu-34.61, Nb-12.88, Al-40.85, Cr-2.89 and Fe-8.76 (all in at.%). This result further confirms that Nb and Al are present in the surface deposit as $NbAl_3$ (Nb: Al = 12.88: 40.85 $\approx$ 3: 1). Since $NbAl_3$ is a fairly stable and chemically inert compound, it is not surprising that the surface deposits in the present study are able to retain the dispersoid as pure $NbAl_3$ even after the prolonged exposure of such aluminides in the electrolyte.

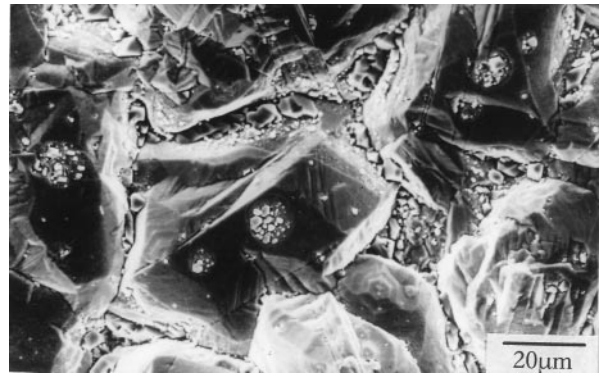

Figure 6. Distribution of codeposited $NbAl_3$ particles both along the grain boundaries as well as within the grain bodies of electrodeposited Cu on pure Cu substrate. Deposition condition was same as that in Fig. 5 except that, $w = 4$ g/l.

Figure 7. Magnified view of Fig. 6 to show that $NbAl_3$ particles are deposited with a varying size distribution from nanocrystalline or submicron size (within grain bodies) to occasionally coarse/agglomerated form (along grain boundaries).

Properties of Surface Deposits

Table 1 summarizes the mechanical (hardness, H_v) and electrical (resistivity, ρ) properties of the surface deposits for different density of colloidal dispersion in the electrolyte during codeposition. It is apparent that average H_v (taken from several regions of the surface deposit) of the codeposited samples undergo a 2.5–4 fold increase than that of the pure Cu substrate. In addition, it is further interesting to note that ρ of the codeposited samples remains nearly identical (same order of magnitude) as that of pure Cu. At higher volume fraction of $NbAl_3$, however, ρ is an order of magnitude higher than that of pure Cu. Thus, increase in H_v with higher than a critical amount or density of $NbAl_3$ may adversely affect the conductivity of the codeposited surface.

Conclusions

It is demonstrated that codeposition of nanocrystalline $NbAl_3$ on Cu substrates is feasible under the present conditions of electrodeposition of Cu. A suitable characterization of the surface microstructure and composition reveals uniform distribution of individual and agglomerated $NbAl_3$ particles along the

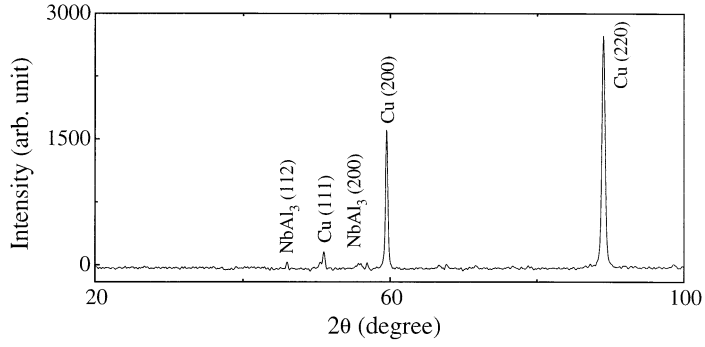

Figure 8. An XRD pattern of a sample surface following codeposition of $NbAl_3$ along with electrodeposition of Cu (from an 8 g/l $CuSO_4$ solution with a pH value of 3.5 and containing colloidal dispersion of 2 g/l of nanocrystalline $NbAl_3$ particles) on pure Cu cathode obtained using Co-K_α radiation. The $NbAl_3$ peaks confirm the presence of these nanocrystalline aluminides on the codeposited surface.

TABLE 1
Results of Hardness and Electrical Resistivity Measurements

Sample	$NbAl_3$ (g/l)	H_v	$\rho(\Omega cm)$
$Cu/NbAl_3$	2	215	7.81×10^{-6}
	3	293	8.86×10^{-6}
	4	340	1.06×10^{-5}
Pure Cu	–	84	1.58×10^{-6}

grain bodies and grain boundaries of electrodeposited Cu, respectively. Following proper codeposition, average microhardness of Cu increases by 2.5–4 fold without adversely affecting its electrical conductivity.

Acknowledgment

Partial financial support from the AICTE Career Award to I.M. and QIP Research Fellowship to P.P.C. are gratefully acknowledgment.

References

1. E. G. West, Copper and Its Alloys, p. 125, Ellis Harwood, Chichester (1982).
2. P. J. Blau (chairman), in ASM Handbook, vol. 18, p. 175, ASM International, Materials Park, OH (1992).
3. I. Manna, J. Dutta Majumder, U. K. Chatterjee, and A. K. Nath, Scripta Mater. 35, 405 (1996).
4. R. R. Oberle, M. R. Scanion, R. C. Cammarata, and P. C. Searson, Appl. Phys. Lett. 66, 19 (1995).
5. A. Guiner, X-ray Diffraction, p. 124, Freeman, San Francisco (1963).
6. Z. Peng, C. Suryanarayan, and F. H. Froes, Metall. Trans. A. 27, 41 (1996).
7. B. D. Cullity, Elements of X-ray Diffraction, p. 102, Addison Wesley, Reading, MA (1975).
8. N. V. Ageev, in Handbook of Binary Metallic Systems, vol. 1, pp. 227–228, Israel Program for Scientific Translation, Jerusalem (1967).